Research Article | Vol. 26, No. 13 | 25 Jun 2018 | OPTICS EXPRESS 17227
Optics EXPRESS

Restriction on orbital angular momentum distribution: a role of media in vortex beams propagation

TAO ZHANG,[1] YI-DONG LIU,[1,*] KUO YANG,[2] JIANDONG WANG,[1] PUSHENG LIU,[1] AND YUANJIE YANG,[1,3,4]

[1] *School of Physics, University of Electronic Science and Technology of China, Chengdu 610054, China*
[2] *Institute of Applied Physics, A'Ba Teachers University, Wenchuan 623002, China*
[3] *School of Astronautics and Aeronautics, University of Electronic Science and Technology of China, Chengdu 611731, China*
[4] *dr.yang2003@uestc.edu.cn*
[*] *liuyd@uestc.edu.cn*

Abstract: The vortex beam carrying single orbital angular momentum (OAM) propagating through a medium with a certain transmission function is investigated. We show that the OAM mode weights in the output OAM spectrum involve two factors: the radial distribution of output beam power and the proposed restriction-characterized function. Based on the restriction-characterized function, we show that the OAM mode weights can only vary in a limited range. We analyze the relationship between the radial distribution of the output beam power and the OAM mode weights in the output OAM spectrum. Finally, our theoretical analysis is illustrated numerically with the cases of eccentric circular aperture and atmospheric turbulence in a weak fluctuation regime. These results provide new insights into the characterization of the OAM spectrum and may find applications for fields involving OAM, such as an OAM-based optical communication link and object detection.

OCIS codes: (050.4865) Optical vortices; (010.3310) Laser beam transmission; (260.0260) Physical optics; (270.0270) Quantum Optics.

References and links

1. L. Allen, M. W. Beijersbergen, R. J. C. Spreeuw, and J. P. Woerdman, "Orbital angular momentum of light and the transformation of Laguerre-Gaussian laser modes," Phys. Rev. A **45**(11), 8185–8189 (1992).
2. A. M. Yao, and M. J. Padgett, "Orbital angular momentum: origins, behavior and applications," Adv. Opt. Photon. **3**, 161–204 (2011).
3. A. E. Willner, H. Huang, Y. Yan, Y. Ren, N. Ahmed, G. Xie, C. Bao, L. Li, Y. Cao, Z. Zhao, J. Wang, M. P. J. Lavery, M. Tur, S. Ramachandran, A. F. Molisch, N. Ashrafi, and S. Ashrafi, "Optical communications using orbital angular momentum beams," Adv. Opt. Photon. **7**, 66–106 (2015).
4. G. Gibson, J. Courtial, M. J. Padgett, M. Vasnetsov, V. Pas'ko, S. M. Barnett, and S. Franke-Arnold, "Free-space information transfer using light beams carrying orbital angular momentum," Opt. Express **12**(22), 5448–5456 (2004).
5. J. Wang, J. Y. Yang, I. M. Fazal, N. Ahmed, Y. Yan, H. Huang, Y. Ren, Y. Yue, S. Dolinar, M. Tur and A. E. Willner, "Terabit free-space data transmission employing orbital angular momentum multiplexing," Nat. Photonics **6**, 488–496 (2012).
6. C. Paterson, "Atmospheric Turbulence and Orbital Angular Momentum of Single Photons for Optical Communication," Phys. Rev. Lett. **94**, 153901 (2005).
7. N. Uribe-Patarroyo, A. Alvarez-Herrero, A. L. Ariste, A. A. Ramos, T. Belenguer, R. M. Sainz, C. LeMen, and B. Gelly, " Detecting photons with orbital angular momentum in extended astronomical objects: application to solar observations," Astronom. Astrophys. **56**, A526 (2011).
8. M. P. J. Lavery, F. C. Speirits, S. M. Barnett, M. J. Padgett, "Detection of a Spinning Object Using Light's Orbital Angular Momentum," Science **341**, 537–540 (2013).
9. S. Furhapter, A. Jesacher, S. Bernet, and M. Ritsch-Marte, "Spiral phase contrast imaging in microscopy," Opt. Express **13**(3), 689–694 (2005).
10. D. G. Grier, "A Revolution in Optical Manipulation," Nature **424**, 21–27 (2003).
11. Y. Yan, G. Xie, M. P.J. Lavery, H. Huang, N. Ahmed, C. Bao, Y. Ren, Y. Cao, L. Li, Z. Zhao, A. F. Molisch, M. Tur, M. J. Padgett, and A. E. Willner, "High-capacity millimetre-wave communications with orbital angular momentum

#325806 https://doi.org/10.1364/OE.26.017227
Journal © 2018 Received 13 Mar 2018; revised 12 May 2018; accepted 6 Jun 2018; published 20 Jun 2018

Optics EXPRESS

multiplexing," Nat. Commun. **5**, 4876 (2014).
12. S. Sasaki, and I. McNulty, "Proposal for Generating Brilliant X-Ray Beams Carrying Orbital Angular Momentum," Phys. Rev. Lett. **100**(12), 124801 (2008).
13. J. A. Anguita, M. A. Neifeld, and B. V. Vasic, "Turbulence-induced channel crosstalk in an orbital angular momentum-multiplexed free-space optical link," Appl. Opt. **47**(13), 2414–2429 (2008).
14. F. Schlederer, M. Krenn, R. Fickler, M. Malik, and A. Zeilinger, "Cyclic transformation of orbital angular momentum modes," New J. Phys. **18** 043019 (2016).
15. Z. Zhu, W. Gao, C. Mu, and H. Li, "Reversible orbital angular momentum photon-phonon conversion," Optica **3**(2) 212–217 (2016).
16. M. Uchida, and A. Tonomura, "Generation of electron beams carrying orbital angular momentum," Nature **464**, 737–739 (2010).
17. R. Liu, D. B. Phillips, F. Li, M. D. Williams, D. L. Andrews, and M, J, Padgett, "Discrete emitters as a source of orbital angular momentum," J. Opt. **17**, 045608 (2015).
18. G. Molina-Terriza, L. Rebane, J. P. Torres, L. Torner, and S. Carrasco, "Probing canonical geometrical objects by digital spiral imaging," J. Europ. Opt. Soc. Rap. Publ. **2**, 07014 (2007).
19. Y. Yang, G. Thirunavukkarasu, M. Babiker, and J. Yuan, "Orbital-Angular-Momentum Mode Selection by Rotationally Symmetric Superposition of Chiral States with Application to Electron Vortex Beams," Phys. Rev. Lett. **119**, 094802 (2017).
20. C. W. Qiu, and Y. Yang, "Vortex generation reaches a new plateau," Science **357**(6352), 645 (2017).
21. L. Torner, J. P. Torres, and S. Carrasco, "Digital spiral imaging," Opt. Express **13**(3), 873–881 (2005).
22. Y. Zhu, L. Zhang, Z. Hu, and Y. Zhang, "Effects of non-Kolmogorov turbulence on the spiral spectrum of Hypergeometric-Gaussian laser beams," Opt. Express **23**(7), 9137–9146 (2015).
23. T. Zhang, Y. D. Liu, J. Wang, P. Liu, and Y. Yang, "Self-recovery effect of orbital angular momentum mode of circular beam in weak non-Kolmogorov turbulence," Opt. Express **24**(18), 20507–20514 (2016).
24. L. C. Andrews, and R. L. Phillips, *Laser Beam Propagation Through Random Media* (SPIE, 2005).
25. I. S. Gradshteyn, and I. M. Ryzhik, *Table of Integrals, Series and Products*, 6th ed. (Academic, 2000).

1. Introduction

A vortex beam can carry orbital angular momentum (OAM) of $l\hbar$ per photon due to its particular phase distribution described by $\exp(\mathrm{i}l\varphi)$, where φ is the azimuthal angle and l is an integer number [1, 2]. In recent decades, many studies have demonstrated that vortex beams have dramatic potential in a wide range of optical applications such as optical communications [3–6], astrophysical observations [7, 8], optical microscopy [9] and optical manipulation [10]. Moreover, the ubiquitous vortices were found and explored for applications in the millimetre-wave and x-ray bands as well as near and in the visible light band [11, 12].

It is well known that the power on OAM modes of light beam may be redistributed when the beam propagates through a medium [13–18]. This redistribution is jointly determined by both the transmission medium and the incident light beam. In OAM multiplexed free-space optical link, compensating the atmospheric turbulence and selecting proper light beam are two effective ways to alleviate the OAM spreading and the resulting crosstalk [6, 13]. By utilizing media with proper properties and shapes, beam power redistribution on OAM modes can be regulated for OAM transformation [14, 15] and for generation of light beams carrying definite OAM [16, 17]. Moveover, information of media can be detected by analyzing the OAM spectrum of distorted wavefront of input vortex beams [18].

The goal of this study is to unveil a rule that how a transmission medium with certain transmission function influences the OAM mode weights of output light beam and we show that the input vortex beam carrying single OAM can only determine these weights within a limited range. In this work, we firstly derive the upper and lower bounds of each OAM mode weight in output OAM spectrum by defining a restriction-characterized function, which is also used to analyze the regularity of the output OAM mode weights varying with radial distribution of normalized output beam power. Indeed, it is not difficult to obtain this novel function because only transmission function is required. For this reason, the restriction exists commonly. In order to show the meaning of our analysis, we illustrate it in two typical examples: eccentric circular hole and the atmospheric turbulence in weak fluctuation regime. Our expectation is to provide, not only a new understanding of how media impact OAM carried by vortex beams, but also

Optics EXPRESS

a useful guide for OAM related applications such as OAM based communication [3], object detection [18] and efficient OAM generation [17, 19, 20].

2. Theoretical analysis

Consider the model establishment which starts with a general expression. With certain transmission function, the normalized complex amplitude function of a vortex beam carrying single OAM propagating along z axis through a medium can be expressed in cylindrical coordinates as

$$\Phi(r,\varphi,z)=\Pi(r,\varphi)R_{l_0}(r,z)\frac{\exp(\mathrm{i}l_0\varphi)}{\sqrt{2\pi}}, \tag{1}$$

where $\Pi(r,\varphi)$ is the transmission function which can be random or not. $R_{l_0}(r,z)$ is the normalized radial basis set, where l_0 is the OAM number. Definitely, $\Phi(r,\varphi,z)$ can be expanded as a superposition of spiral harmonics [21]

$$\Phi(r,\varphi,z)=\frac{1}{\sqrt{2\pi}}\sum_{l=-\infty}^{\infty}C_l(r,z)\exp(\mathrm{i}l\varphi). \tag{2}$$

Because of the orthogonality of spiral harmonics, the coefficient $C_l(r,z)$ can be expressed as

$$C_l(r,z)=\frac{1}{2\pi}\int_0^{2\pi}\Pi(r,\varphi)R_{l_0}(r,z)\exp(-\mathrm{i}\Delta l\varphi)\mathrm{d}\varphi, \tag{3}$$

where $\Delta l=l-l_0$. In previous work, the rotational coherence function of phase perturbations in the atmospheric turbulence was investigated [6]. Here we shall refer to $\langle\Pi(r,\varphi_1)\,[\Pi(r,\varphi_2)]^*\rangle$ as the rotational coherence function of both phase and amplitude perturbations, and subsequently express its circular harmonic transform as

$$A_{\Delta l}(r)=\frac{1}{4\pi^2}\int_0^{2\pi}\int_0^{2\pi}\langle\Pi(r,\varphi_1)\,[\Pi(r,\varphi_2)]^*\rangle\exp[-\mathrm{i}\Delta l(\varphi_1-\varphi_2)]\mathrm{d}\varphi_1\mathrm{d}\varphi_2, \tag{4}$$

where $\langle\cdot\rangle$ is the ensemble average corresponding to random medium. $A_{\Delta l}(r)$ reflects the impact of media on the radial distribution of incident beam power on the OAM mode with Δl. In Eq. (4), the real function $A_{\Delta l}(r)\geq 0$ and in the circular symmetric media, $A_{\Delta l\neq 0}(r)$=0. Calculating ensemble average is a convenient way to investigate the OAM mode weights of output beam through a random medium such as the atmospheric turbulence [6, 22, 23]. Based on [21], we express the OAM mode weight of l with the ensemble average for both random and non-random media as

$$p_l(z)=\frac{\int_0^{\infty}\langle|C_l(r,z)|^2\rangle r\mathrm{d}r}{\sum_{\Delta l=-\infty}^{\infty}\int_0^{\infty}\langle|C_l(r,z)|^2\rangle r\mathrm{d}r}. \tag{5}$$

Since $\langle|C_l(r,z)|^2\rangle=|R_{l_0}(r,z)|^2A_{\Delta l}(r)$, the OAM mode weight of l reads

$$p_l(z)=\frac{\int_0^{\infty}|R_{l_0}(r,z)|^2A_{\Delta l}(r)r\mathrm{d}r}{\int_0^{\infty}|R_{l_0}(r,z)|^2\sum_{\Delta l=-\infty}^{\infty}A_{\Delta l}(r)r\mathrm{d}r}. \tag{6}$$

Here we define a restriction-characterized function of medium as

$$\Omega_{\Delta l}(r)=\frac{A_{\Delta l}(r)}{\sum_{\Delta l=-\infty}^{\infty}A_{\Delta l}(r)}, \tag{7}$$

where it is provable that $0\leq\Omega_{\Delta l}(r)\leq 1$. In Eq. (7), $\Omega_{\Delta l}(r)$ for each Δl is completely determined by media, showing the restriction on output OAM mode weight distribution. The denominator

Optics EXPRESS

$\sum_{l=-\infty}^{\infty} A_{\Delta l}(r)$ in Eq. (7) reflects the impact of media on the power radial distribution of incident light beam. The denominator being smaller than, equal to and higher than 1 means that the power radial density is weakened, unchanged and strengthened, respectively. The denominator of $\Omega_{\Delta l}(r)$ mathematically should not be 0, and thus the discussion of $\Omega_{\Delta l}(r)$ requires r to be limited into the region S where $\sum_{l=-\infty}^{\infty} A_{\Delta l}(r) \neq 0$. It is provable that the $p_l(z)$ in Eq. (6) can also be expressed as an inner product in the region S

$$p_l(z) = \int_S \Psi(r, z)\Omega_{\Delta l}(r)\mathrm{d}r, \tag{8}$$

where

$$\Psi(r, z) = \frac{|R_{l_0}(r, z)|^2 \sum_{\Delta l=-\infty}^{\infty} A_{\Delta l}(r) r}{\int_S |R_{l_0}(r, z)|^2 \sum_{\Delta l=-\infty}^{\infty} A_{\Delta l}(r) r \mathrm{d}r}. \tag{9}$$

Properties of vortex beams such as OAM number, frequency and other parameters were emphatically investigated when the effects of media such as the atmospheric turbulence on the OAM of vortex beams were studied in previous work [22, 23]. Equation (8) shows that the OAM weight $p_l(z)$ only depends on two parts: $\Psi(r, z)$ and the restriction-characterized function $\Omega_{\Delta l}(r)$. $\Psi(r, z)$ is the radial distribution of normalized output beam power where $\int_S \Psi(r, z)\mathrm{d}r$=1. Since $\Omega_{\Delta l}(r)$ with each Δl is only determined by the properties of media, for a given Δl, the reason for why l_0 and frequency can impact $p_l(z)$ is just that they can impact $\Psi(r, z)$. In order to be more essential, in the following discussion, we only discuss the impacts of the two parts rather than other factors on output OAM weight.

Since $\int_S \Psi(r, z)\mathrm{d}r$=1, $p_l(z)$ can be viewed as an expected value where $\Psi(r, z)$ is the probability density function of $\Omega_{\Delta l}(r)$. Normally, at an arbitrary r, $\Psi(r, z)$ increases as the radial distribution of input beam power $|R_{l_0}(r, z)|^2 r$ increases. In particular, if $\sum_{l=-\infty}^{\infty} A_{\Delta l}(r)$ is a constant, $\Psi(r, z)$ is reduced to $|R_{l_0}(r, z)|^2 r$. Equation (8) implies that, to obtain larger weight of the OAM mode with arbitrary Δl in output OAM spectrum, the output beam power should concentrate close to the radial position with larger $\Omega_{\Delta l}(r)$.

Another meaningful result is that, if the supremum $\sup\{\Omega_{\Delta l}(r)\}$ and the infimum $\inf\{\Omega_{\Delta l}(r)\}$ exist, then

$$\inf\{\Omega_{\Delta l}(r)|r \in S\} \leq p_l(z) \leq \sup\{\Omega_{\Delta l}(r)|r \in S\}. \tag{10}$$

Equation (10) quantifies the upper and lower bounds of OAM mode weight $p_l(z)$. When transmission function is explicit, both of these bounds for each Δl are fixed. Note that the maximum value $[\Omega_{\Delta l}(r)]_{\max}$ and the minimum value $[\Omega_{\Delta l}(r)]_{\min}$, if exist, are definitely equal to $\sup\{\Omega_{\Delta l}(r)|r \in S\}$ and $\inf\{\Omega_{\Delta l}(r)|r \in S\}$, respectively. In general, $p_l(z)$ is between the two bounds and can be impacted by the input vortex beam. But in some particular cases, e.g., in case of the free space ($\Pi(r, \varphi) = 1$ and thus $\inf\{\Omega_{\Delta l}(r)|r \in S\} = \sup\{\Omega_{\Delta l}(r)|r \in S\} = 1$), input vortex beams has no impact on $p_l(z)$ which reaches both of bounds. The propagation distance z in $p_l(z)$ is only associated with the amplitude distribution of vortex beams, and we only consider the case of z=0 in the following discussion.

3. Discussion of typical examples

Based on the above analysis, as the first example, we investigate the restriction of a misaligned optical element on output OAM distribution. Here we simply consider a transverse obstruction with an eccentric circular hole placed in the propagation path of a vortex beam. The transmission function of the obstruction can be written as $\Pi(r, \varphi) = 1\ ((r/R)^2 + (r_0/R)^2 - 2(r/R)(r_0/R)\cos(\varphi - \varphi_0) \leq 1)$ or 0 (other cases), where $R > 0$ is the radius of the circular hole. (r_0, φ_0) is the place of

Optics EXPRESS

centre of the circular hole in polar coordinates. Consequently, the $\Omega_{\Delta l}(r)$ of an eccentric circular hole reads

$$\Omega_{\Delta l}(r) = \begin{cases} \dfrac{\Delta\theta^2}{\Delta\theta^2 + 4\sum_{n=1}^{\infty}\frac{1-\cos(n\Delta\theta)}{n^2}} & (\Delta l = 0) \\ \dfrac{2[1-\cos(\Delta l\Delta\theta)]}{\Delta l^2\Delta\theta^2 + 4\Delta l^2\sum_{n=1}^{\infty}\frac{1-\cos(n\Delta\theta)}{n^2}} & (\Delta l \neq 0). \end{cases} \tag{11}$$

In Eq. (11), the expression of $\Delta\theta$ ($0 \sim 2\pi$) depends on the relation of circular area with the radius r and the center at the optical axis to the hole area. If the circular area is completely in the hole area, $\Delta\theta = 2\pi$ and consequently $\Omega_{\Delta l}(r)$=1 ($\Delta l = 0$) or 0 ($\Delta l \neq 0$). If it is partially in the hole area, $\Delta\theta = 2\arccos[(r_0/r + r/r_0 - R^2/r_0 r)/2]$. If it is completely outside of the hole area, $\Delta\theta = 0$ and consequently $\Omega_{\Delta l}(r)$ is meaningless. It can be known in Eq. (11) that, both bounds for each Δl only depends on the eccentric coefficient r_0/R. Based on Eq. (11), the upper and lower bounds of OAM mode weights with $\Delta l = 0,\ 1$ in output OAM spectrum are plotted in Fig. 1 as functions of r_0/R.

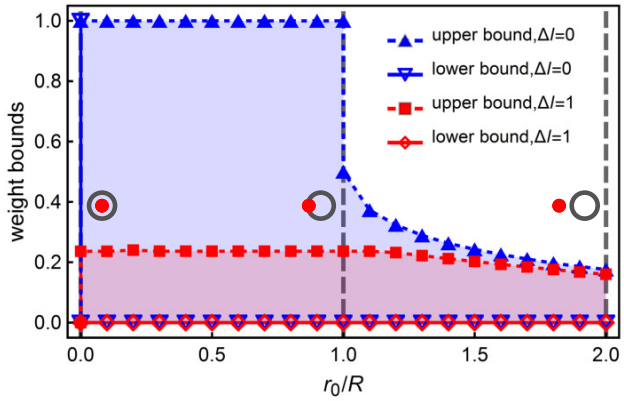

Fig. 1. Upper and lower bounds of output OAM mode weights for $\Delta l = 0, 1$ (defined by Eq. (10)) in the case of eccentric circular hole against the eccentric coefficient r_0/R. There are indications of relative position between the optical axis (•) and the hole edge (◯) for $r_0/R = 0, 1, 2$, respectively.

As can be seen, the curves of both the bounds, with discontinuity, show non-smooth change of varying ranges of the OAM mode weights as r_0/R grows. The hole is circularly symmetric with no misalignment ($r_0/R = 0$), and all the vortex beams can completely reserve their symmetrical patterns through it. Therefore, both bounds for $\Delta l = 0$ and $\Delta l = 1$ are 1 and 0, respectively, which indicates that the weight of initial OAM mode keeps 1 regardless of the properties of the input beam. As misalignment arises ($r_0/R > 0$), the OAM mode weights can be changed because of difference of values between the two bounds. In this case, lower bounds for all Δl are 0 because $\inf\{\Omega_{\Delta l}(r)|r \in S\} = \lim_{\Delta\theta\to 0}\Omega_{\Delta l}(r) = 0$. When optical axis locates in the hole area with misalignment ($0 < r_0/R < 1$), it is provable in Eq. (11) that the upper bounds for all Δl are invariable. Here the fixed upper bounds $\sup\{\Omega_{\Delta l=0}(r)|r \in S\} = 1$ and $\sup\{\Omega_{\Delta l=1}(r)|r \in S\} = 0.236$, with their zero lower bounds, show the constant and great ranges that the OAM mode weights can vary in. In this case, the more the output beam power concentrates close to the optical axis, the better the symmetrical pattern of initial optical field can be reserved, and thus the weight of initial OAM mode can near 1. But, when optical axis moves

Optics EXPRESS

outside of the hole ($r_0/R > 1$), no vortex beams can well reserve their symmetrical patterns through it, and thus the upper bound for $\Delta l = 0$ jumps to a low level. Thus, it is not possible to obtain a large weight of initial OAM mode. To avoid the OAM spreading which can not be alleviated to a high level by changing properties of input vortex beam, the eccentric coefficient, enlightened by the simulation results, should be lower than a threshold.

In order to show how output OAM distribution varies with radial distribution of normalized output beam power under $\Omega_{\Delta l}(r)$ in this example, we consider four LG beams with different OAM numbers and different radial indexes propagating through the same eccentric circular hole, as shown in Fig. 2.

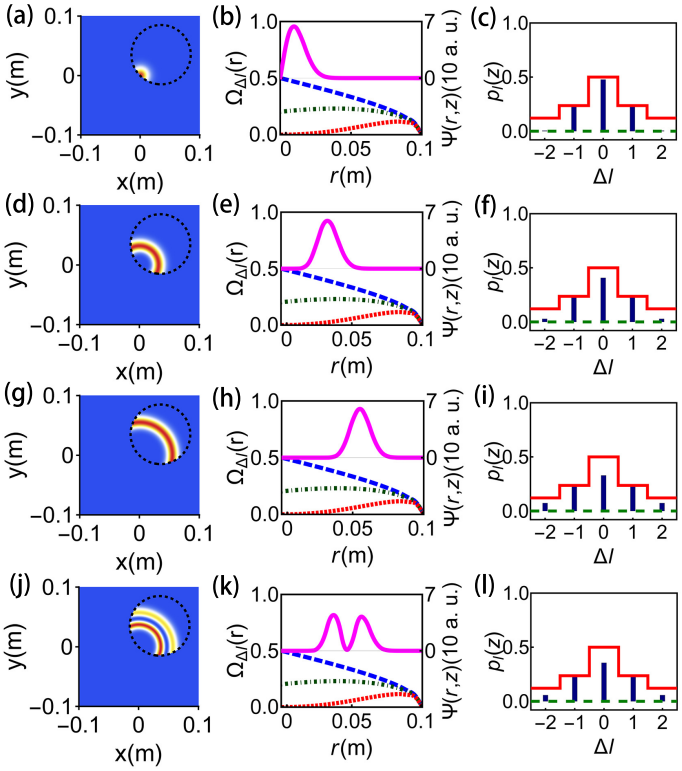

Fig. 2. Restriction of the eccentric circular hole with R=0.05 m and $\{r_0 = 0.05\text{m}, \varphi_0 = \pi/4\}$ upon output OAM distribution of LG beams. There are considerations on the LG mode with l_0=0, radial index p=0 and waist radius 0.02m at z=0: (a) output intensity distribution, where dash black line indicates the hole edge, (b) curves of $\Psi(r, z)$ (solid pink line) and $\Omega_{\Delta l}(r)$ with Δl=0 (long dash blue line), Δl=1 (dot dash green line) and Δl=2 (short dash red line), (c) distribution of output OAM mode weights for $\Delta l = 0$ to 2, along with their upper bounds (solid red line) and lower bounds (dash green line). Moreover, there are considerations of LG modes respectively based on (d)-(f) l_0=5 and p=0, (g)-(i) l_0=15 and p=0, (j)-(l) l_0=10 and p=1.

After passing through an eccentric circular hole with $r_0/R = 1$, four selected LG beams have different output intensity patterns (Fig. 2, left column), which respectively result in four different radial distributions of normalized output beam power plotted by the solid pink curves (Fig. 2, middle column). The fixed transmission function leads to the same curve cluster of $\Omega_{\Delta l}(r)$ in Figs. 2(b), 2(e), 2(h) and 2(k). For each Δl, varying trend of curve of its $\Omega_{\Delta l}(r)$ means a unique restriction, under which a varying regularity of the corresponding OAM mode weight in output

Optics EXPRESS

OAM spectrum in relation to the $\Psi(r, z)$ exists. For example, with the decreasing $\Omega_{\Delta l=0}(r)$, as the output beam power concentrates close to the optical axis, the OAM mode weight for $\Delta l = 0$ increases in the range between lower bound 0 and upper bound 0.5 (Fig. 2, right column). For this, we deduce that, a vortex beam with more concentrated energy can be better to resist OAM spreading in this case. Moreover, the simulation results from the case of $\Delta l = 0$, together with those from the cases of $\Delta l = 1$ and $\Delta l = 2$, are perfectly consistent with the above analysis.

As the second example, we investigate the restriction in the case of the atmospheric turbulence in weak fluctuation regime. There are researches involving the turbulence effects on vortex beams with diverse OAM modes, where the OAM mode weights of output light beam are associated with properties of the input vortex beam [6, 22, 23]. Paterson pointed out that, in this medium, the more the power of input vortex beam distributes close to the optical axis, the larger the detection probability of initial OAM mode can be obtained [6]. Here we explain this phenomenon by the restriction theory and answer a question: where are the bounds of OAM mode weight for each Δl when OAM of a vortex beam spreads in the atmospheric turbulence?

To obtain $\Omega_{\Delta l}(r)$ of the atmospheric medium, derivation will be based on the non-Kolmogorov model which is widely used. In weak fluctuation regime, random phase fluctuation caused by the turbulence is the main cause for OAM spreading [6]. Considering the ensemble average and using the quadratic approximation, then $\langle \Pi(r, \varphi)[\Pi(r, \varphi')]^* \rangle = \exp\{-[2r^2 - 2r^2\cos(\varphi' - \varphi)]/\rho_0^2\}$, where ρ_0 is the spatial coherence radius for a plane or spherical wave in non-Kolmogorov turbulence [24]. By means of the equation $\int_0^{2\pi} \exp[-in\varphi_1 + \eta\cos(\varphi_1 - \varphi_2)]d\varphi_1 = 2\pi \exp(-in\varphi_2) I_n(\eta)$, where $I_n(\cdot)$ is the modified Bessel function of the first kind with order n [25], then

$$\Omega_{\Delta l}(r) = \exp\left(\frac{-2r^2}{\rho_0^2}\right) \mathrm{I}_{\Delta l}\left(\frac{2r^2}{\rho_0^2}\right). \tag{12}$$

After calculating the supremum and the infimum of $\Omega_{\Delta l}(r)$ in Eq. (12), here we found that the upper and lower bounds of OAM mode weights for each Δl are irrelevant to ρ_0 which indicates the strength of phase fluctuation.

To show the varying range of OAM low-order mode weights in output OAM spectrum in this example, the upper bounds are calculated by Eq. (12), as shown in Table 1. The lower bounds for all Δl can be directly calculated by $\inf\{\Omega_{\Delta l}(r) | r \in S\} = \lim_{r \to +\infty} \Omega_{\Delta l}(r) = 0$. These values are intrinsic and unique, because they are independent of any properties of input vertex beam and even the strength of phase fluctuation. The upper bound drops rapidly as $|\Delta l|$ increases. When $|\Delta l| > 2$, as a result of the fixed upper bounds near zero, the probability of an OAM mode being cast into another one is very small.

Table 1. The upper bounds of output OAM mode weights for $|\Delta l|$=0 to 5 (defined by Eq. (10)) in the case of the atmospheric turbulence in weak fluctuation regime.

$\lvert\Delta l\rvert$	0	1	2	3	4	5
upper bound	1	0.219	0.118	0.080	0.060	0.048

The atmospheric turbulence in weak fluctuation regime is transparent, and thus the $\Psi(r, z)$ is reduced to the $|R_{l_0}(r, z)|^2 r$. To show how OAM low-order mode weights in output OAM spectrum vary with $\Psi(r, z)$ under the restriction characterized by $\Omega_{\Delta l}(r)$, three different narrow LG beams are considered. Their beam power distributions keep unchanged in propagation, because here only phase fluctuation needs to be taken into account (see Fig. 3, left column). Still, our restriction analysis can be supported by the simulation results which will be shown next. When distribution of the $\Psi(r, z)$ concentrates around where $\Omega_{\Delta l=0}(r)$ is the maximum, the OAM mode weight with $\Delta l = 0$ in output OAM spectrum approaches its upper bound (see Figs. 3(b) and 3(c)). But with the decreasing $\Omega_{\Delta l=0}(r)$, there is a regularity showing that, as peak of the $\Psi(r, z)$ moves to where

Optics EXPRESS

the $\Omega_{\Delta l=0}(r)$ is smaller (away from the optical axis), the weight decreases (see Figs. 3(c), 3(f) and 3(i)). Therefore, a more concentrated vortex beam can be better to resist OAM spreading that agrees with Paterson's view. The "self-recovery effect" in our previous work [23] exists because the power of a vortex beam with sufficient focusing-ability in propagation can rapidly concentrate around the optical axis where $\Omega_{\Delta l=0}(r)$ is larger, although a larger ρ_0 results in a more rapid decline of $\Omega_{\Delta l=0}(r)$ as the propagation distance becomes longer. In previous work, the results show that the OAM spreading becomes serious as the OAM number of the input vortex beam increases [22,23]. The only reason for this is that, when OAM number increases, the output power of the incident beam moves away from the optical axis.

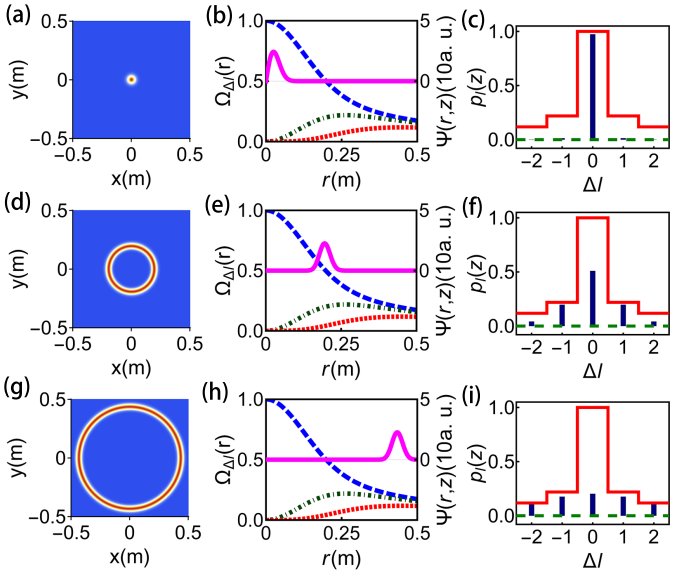

Fig. 3. (a)-(c) Restriction of the atmospheric turbulence in weak fluctuation regime upon output OAM distribution of an input LG beam with l_0=0, p=0, ρ_0=0.3m, waist radius 0.05 m and z=0: (a) output intensity distribution; (b) curves of $\Psi(r, z)$ (solid pink line) and $\Omega_{\Delta l}(r)$ with Δl=0 (long dash blue line), Δl=1 (dot dash green line) and Δl=2 (short dash red line); (c) distribution of output OAM mode weights for Δl = 0 to 2, along with their upper bounds (solid red line) and lower bounds (dash green line). Moreover, there are cases of LG modes based on (d)-(f) l_0=30, (g)-(i) l_0=150, respectively.

4. Conclusion

We have discovered a restriction on OAM mode weights in output OAM spectrum when a vortex beam propagates through a generalized medium. The restriction was studied based on a novel function $\Omega_{\Delta l}(r)$, which was derived from the transmission function. We found a varying regularity of the OAM mode weights in output OAM spectrum in relation to the radial distribution of output beam power under the restriction characterized by the $\Omega_{\Delta l}(r)$. It shows that, as the output beam power concentrates close to the radial position with larger $\Omega_{\Delta l}(r)$, the corresponding OAM mode weight is larger. We also calculated the upper and lower bounds to show the varying range of each OAM mode weight in output OAM spectrum, using the supremum and the infimum of $\Omega_{\Delta l}(r)$, respectively. Besides the media we discussed, one can also consider those of the other kinds, e.g., the medium with a well-structured $\Omega_{\Delta l}(r)$ for OAM generation. Due to the limitation of this work, it is worth to make a more general discussion such as, considering more common incident light beams.

Optics EXPRESS

Funding

National Natural Science Foundation of China (NSFC) (11474048, 60908034, 61205122); Fundamental Research Funds for the Central Universities (ZYGX2013J052, ZYGX2015J042); Scientific Research Fund of Sichuan Provincial Education Department (18ZA0004).